

# Digital micromirror transient response influence on superfast 3D shape measurement

Yajun Wang<sup>a</sup>, Bhaskar Bhattacharya<sup>a</sup>, Eliot H. Winer<sup>a</sup>, Peter Kosmicki<sup>b</sup>,  
Wissam H. El-Ratal<sup>b</sup>, Song Zhang<sup>a,\*</sup>

<sup>a</sup> Mechanical Engineering Department, Iowa State University, Ames, IA 50011, United States

<sup>b</sup> John Deere Product Engineering Center, Waterloo, IA 50704, United States

## ARTICLE INFO

### Article history:

Received 17 October 2013

Received in revised form

4 January 2014

Accepted 18 January 2014

### Keywords:

Digital micromirror device  
Superfast 3D shape measurement  
Binary defocusing  
Phase shifting  
Transient response

## ABSTRACT

Nowadays, the high speed (e.g., kilo-Hertz) refreshing rate of the digital micro-mirror device (DMD) has enabled superfast 3D shape measurement using the binary defocusing technique. This research finds that when the system reaches its extreme binary pattern refreshing rate, the transient response of the DMD induces a coupling effect (i.e., two neighboring patterns blend together) that may cause substantial measurement error. Since this transient response repeats itself, this systematic measurement error is substantially reduced to a negligible level when the timing between the projector and the camera is properly adjusted. Experimental results are presented to demonstrate the observed phenomena, and the success of utilizing the proposed method to overcome the problems associated with the transient response of the DMD.

© 2014 Elsevier Ltd. All rights reserved.

## 1. Introduction

The capture of 3D geometric motion of rapidly changing events is used considerably in academia. This new process started to impact the industry by enabling the acquisition of a new type of data that is vital to the development of new products. For instance, capturing the motion of a live beating heart is vital to understanding its mechanics and physiology [1]. Capturing quantitative measured data of debris flying around agricultural machinery while operating in the field is critical to the development of robust designs. Real-time 3D shape measurement has been realized by adopting the digital fringe projection (DFP) method facilitated by digital light processing (DLP) projectors [2,3]. However, it is extremely difficult for conventional DFP techniques to achieve rates higher than 120 Hz (which is the maximum refresh rate of a digital video projector). Therefore, it is difficult for such techniques to achieve high speed motion capture.

Recent advances in superfast 3D shape measurement have allowed high speed (in the order of kHz or higher) measurement rates by utilizing coherent laser interference and rotating mirrors [4], LED projection arrays [5], and digital binary pattern projection by the digital light processing (DLP) projectors [6]. All these technologies have utilized phase-shifting algorithms to achieve

high-spatial resolution. The laser interference based technology [4] has the issue associated with the coherent lasers: speckle noise, albeit they partially reduced this problem by adding a second camera. The LED projection system [5] could reach 100 kilo-Hertz (kHz), yet the system they developed only reached 47 Hz due to the camera they used, and possibly the brightness of the projectors and some transient response of the LED light used. We have successfully developed a system [6] that could achieve 32 kHz using the DLP Discovery platform and the binary defocusing technique [7]. However, the core of the DLP technology is the digital micro-mirror device (DMD) that is inherently a mechanical device that toggles the pixel ON or OFF by mechanically flipping the micro-mirrors from one position to the other. This transient response of the digital micro-mirrors could influence the measurement quality as well if its speed limit is reached.

The binary defocusing technique has enabled us to achieve high speed (in the order of tens of kHz) 3D shape measurement because it requires only 1-bit structured patterns rather than 8-bit grayscale patterns [6]. However, the measurement error is large if the projector is not properly defocused [8]. Techniques based on 1-D pulse width modulation (PWM) [9–14], 2D area modulation [15,16], and binary dithering [17] as well as the optimized dithering techniques [18,19] have been developed to improve the binary defocusing technique. They proved successful in attaining high-quality 3D shape measurement even if the projector is nearly focused; and if the projector is slightly defocused, the phase quality obtained from the binary patterns could be the same as that

\* Corresponding author. Tel.: +1 515 294 0723; fax: +1 515 294 3261.  
E-mail address: [song@iastate.edu](mailto:song@iastate.edu) (S. Zhang).

obtained from the traditional sinusoidal fringe patterns. Our prior knowledge tells us on how to reduce the phase measurement error to a negligible level caused by the binary defocusing itself. Therefore, the phase measurement error discussed in this paper is mainly caused by sources other than the defocused binary patterns.

This paper presents a new phenomena that we have never observed before for superfast 3D shape measurement. Our experiments find that even if the binary patterns are properly selected and defocused, significant phase measurement error still occurs if the high-speed projectors (e.g., DLP LightCommander and DLP LightCrafter) operate under the structured light mode and pattern switching rate is at its maximum with the maximum illumination time. We discover that the transient response of the DMD causes pattern coupling (i.e., two neighboring patterns blend together) when the projector operates under the aforementioned conditions. Further experiments find that the transient response is a systematic error (i.e., an error caused independent of the projection speed), and thus its influence on phase measurement error could be reduced if the proper method is developed. This paper presents a method that we have developed to mitigate this problem by changing the timing of the system: the exposure time of the projector, the starting time and exposure time of the camera. We will demonstrate that this method can reduce the phase measurement error to a negligible level.

Section 2 explains the principles of proposed techniques. Section 3 shows some experimental results, and Section 4 summarizes the paper.

## 2. Principle

### 2.1. Two-frequency phase-shifting technique for absolute phase retrieval

Phase-shifting methods have been extensively adopted in optical metrology because of their measurement speed and accuracy. Over the years, a variety of phase-shifting algorithms have been developed, that include three-step, four-step, and least-square algorithms [20]. For high-speed 3D shape measurement, a three-step phase-shifting algorithm with a phase shift of  $2\pi/3$  is commonly used. The three fringe images can be described as

$$I_1(x, y) = I'(x, y) + I''(x, y) \cos(\phi - 2\pi/3), \quad (1)$$

$$I_2(x, y) = I'(x, y) + I''(x, y) \cos(\phi), \quad (2)$$

$$I_3(x, y) = I'(x, y) + I''(x, y) \cos(\phi + 2\pi/3). \quad (3)$$

where  $I'(x, y)$  is the average intensity,  $I''(x, y)$  the intensity modulation, and  $\phi(x, y)$  the phase to be solved for. Simultaneously solving Eqs. (1)–(3), the phase can be obtained

$$\phi(x, y) = \tan^{-1}[\sqrt{3}(I_1 - I_3)/(2I_2 - I_1 - I_3)]. \quad (4)$$

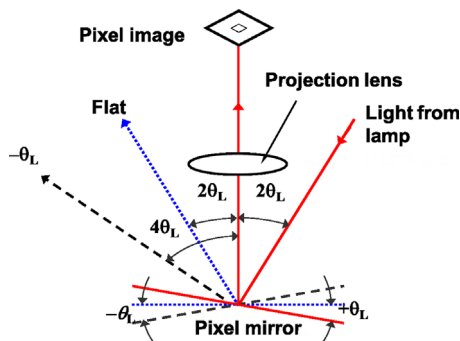


Fig. 1. Optical switching principle of a digital micro-mirror device (DMD).

This equation provides the wrapped phase with  $2\pi$  discontinuities. A spatial or temporal phase unwrapping algorithm can be applied to obtain continuous phase.

We utilized a two-frequency temporal phase-unwrapping algorithm to unwrap the phase. Essentially, two wrapped phase maps, low frequency phase  $\phi^l(x, y)$  and high-frequency  $\phi^h(x, y)$  were used.  $\phi^l(x, y)$  is obtained from wide fringe patterns with a single fringe covering the whole measuring range, such that no phase unwrapping is required. By referring to  $\phi^l(x, y)$  point by point,  $\phi^h(x, y)$  is unwrapped to obtain a continuous phase map,  $\Phi(x, y)$ . Because 3D information (i.e., the depth) is carried on by the phase, 3D shape can be reconstructed from the unwrapped phase  $\Phi(x, y)$  using a phase-to-height conversion algorithm [8].

### 2.2. Fundamentals of the DLP technology

Digital light processing (DLP) concept originated from Texas Instruments (TI) in the later 1980s. TI began its commercialized DLP technology in 1996. At the heart of every DLP projection system is an optical semiconductor called the digital micro-mirror device (DMD), which functions as an extremely precise light switch. The DMD chip contains an array of hinged, microscopic mirrors, each of which corresponds to 1 pixel of light in a projection image.

Fig. 1 shows the working principle of the micro mirror. The micro mirror can be moved to  $+\theta_L$  (ON) or  $-\theta_L$  (OFF), thereby modulating the output light corresponding to that cell. The rate of a mirror switching ON and OFF determines the brightness of the projected image pixel. Gray-scale values are produced by controlling the proportion ON and OFF times of the mirror during one projection period (black being 0% ON time and while white being 100% ON time).

### 2.3. Fundamentals of the binary defocusing technique

For a conventional DFP technique, sinusoidal patterns are projected and captured for 3D information extraction. Since it requires to project 8-bit sinusoidal patterns, the refresh rate of a digital video projector is typically limited to 120 Hz, which is not sufficient for high-speed motion measurement. The recently proposed binary defocusing technique is able to break the speed limitation for DFP technique. Instead of sending 8-bit sinusoidal patterns, 1-bit binary patterns are fed to the projector. By properly defocusing the projector, the projected patterns will be pseudo-sinusoidal. Fig. 2 shows the results with different defocusing levels. The first row of Fig. 2 shows the captured defocusing binary patterns, while the second row of Fig. 2 shows the corresponding cross sections.

Since only 1-bit binary patterns are used, there are some techniques which can be used for high-speed pattern projection. For example, the DLP LightCommander projector can switch binary patterns at 4 kHz, while it can only project sinusoidal patterns at about 700 Hz. By using the binary defocusing technique, we have demonstrated the feasibility for superfast motion capture [6]. However, when operating under high speed, there are limitations for some projectors, which may bring error to the final measurement result. In the following sections of this paper, we will demonstrate the limitation of a DLP LightCommander projector along with our proposed solution.

## 3. Experiments

### 3.1. Experimental system setup

The developed 3D shape measurement system is composed of a DLP LightCommander projector (model: LightCommander,

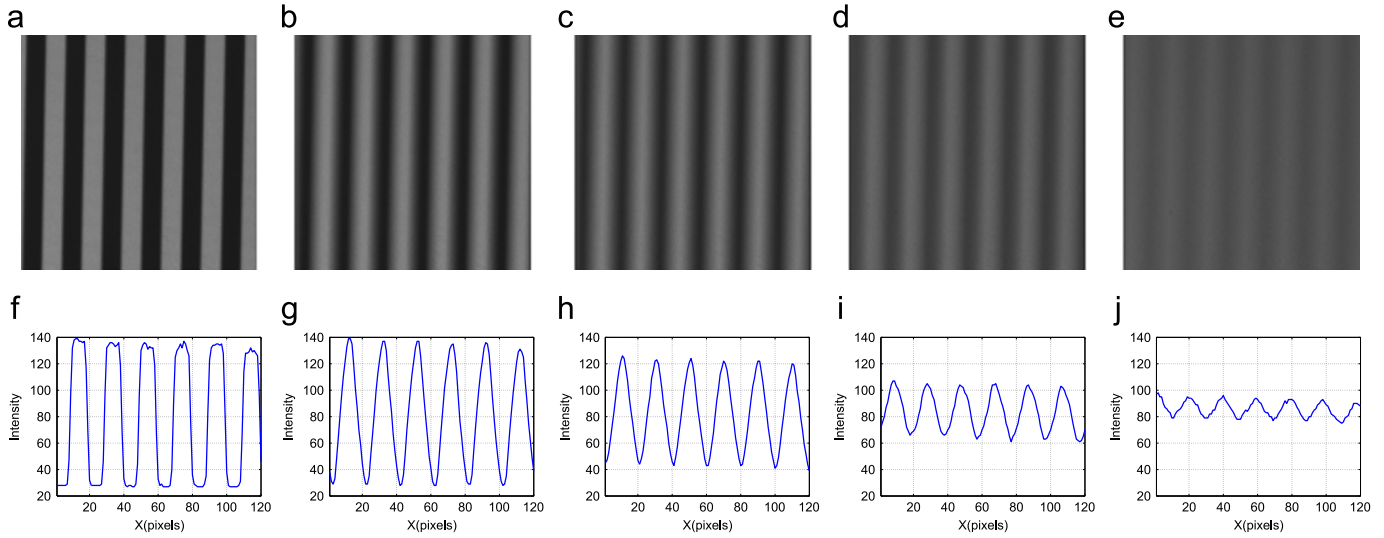


Fig. 2. Binary defocusing patterns with different defocusing levels.

LogicPD, MN), a high-speed CMOS camera (model: Phantom V9.1, Vision Research, NJ). The projector contains a high performance light engine comprised of a core optical module and the LED illumination modules. It is capable for binary pattern projection up to 4 kHz, with a  $1024 \times 768$  resolution. The camera offers 1016 frames per second (fps) at a full resolution of  $1632 \times 1200$  pixels, up to 153,846 fps maximum. In our experiments, we used a  $576 \times 576$  image resolution. The synchronization circuit takes the projection timing signal and sends the trigger signal to the camera for simultaneous image acquisition. Both of the projector and the camera are attached with a Nikon 50 mm f/1.8 AF lens. Fig. 3 shows the system that was developed. The distance between the projector and the camera is about 310 mm.

The experimental results we will present are all based on the LogicPD LightCommander projector. However, our investigation on other high-speed DLP projectors (i.e., DLP LightCrafter 3000 and DLP LightCrafter 4500, Texas Instruments, TX) also observed similar phenomena, albeit at different significance levels. Therefore, the findings in this research are not limited to the DLP LightCommander projector.

### 3.2. Transient response of the DMD with binary image input

In our previous research, we found that when the DLP LightCommander projector operates under a high speed (kHz) with the maximum exposure time, the patterns captured by a well synchronized high-speed camera will be coupled with adjacent frames. Since the phase information is extracted from several adjacent patterns, the coupling effect will cause phase errors. In order to understand the transient response of the DMD of the LightCommander projector, we carried out a simple experiment by placing a photodiode (model: Thorlabs FDS100; with a resistor:  $30 \text{ K}\Omega$ ) in front of the projector. Care was taken that the photodiode was not placed too close to the projector where reflections become an issue or too far where the intensity of light was too dim. An oscilloscope (model: Tektronix TDS2024B) was used to visualize and record the signal of the photodiode system as the projector projected patterns under different speeds and illumination times.

In this experiment, two patterns of pure white and pure black were alternately sent to the projector. In an ideal case, a periodic square wave should be observed. During the white (first half) projection cycle the response should be high while during the black (second half) projection cycle, the response

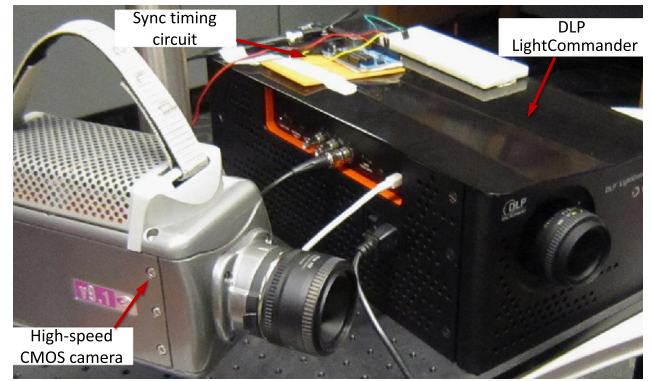
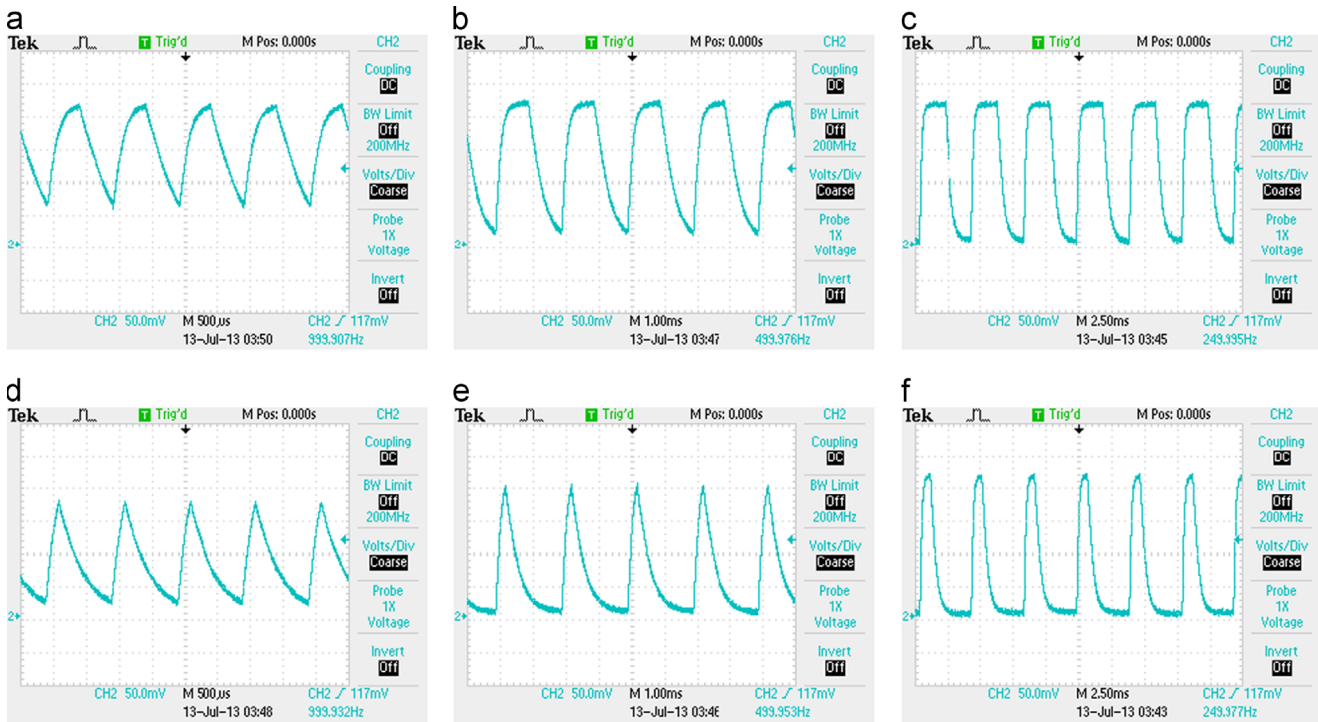


Fig. 3. The 3D shape measurement system.

should fall immediately to zero. In other words, the recorded voltage signal should be as close to a square wave as possible. However, the voltage signals recorded under different projection speeds and illumination times as shown in Fig. 4 are not ideal, which reveal the complex transient response of the DMD.

Fig. 4(a)–(c) shows the results of respectively 2 kHz, 1 kHz, and 500 Hz with their maximum allowed illumination time ( $494 \mu\text{s}$ ,  $994 \mu\text{s}$ , and  $1994 \mu\text{s}$ ). Fig. 4(d)–(f) shows the corresponding results by using a shorter illumination time ( $200 \mu\text{s}$ ,  $300 \mu\text{s}$ , and  $800 \mu\text{s}$ ). As per Fig. 4(a)–(c), we find if the maximum illumination time is used, when the projection pattern is switched from white to black, the DMD chips require a long time to respond by toggling to the off position. This effect which we term as a *coupling effect* is especially evident with projection speeds of over 1 kHz since the projected light is not able to fall to zero. However, if we use a shorter illumination time, the results begin to show improvement as shown in Fig. 4(d)–(f). Take the result in Fig. 4(f) as an example, in the white projection cycle, the DMD chips toggle on for half the cycle and before the next half cycle, they have enough time to toggle off. Therefore, for the adjacent black cycle, the DMD chips always toggle off. In this way, if the camera is well synchronized with the projector, the captured patterns will have no coupling effects. It is worthwhile to note that, for the experiments in the following sections, the projector was set and compared at the same conditions with this section.





**Fig. 4.** Transient responses of the DMD of DLP LightCommander projector. (a) 2 kHz projection rate with 494  $\mu$ s illumination time; (b) 1 kHz projection rate with 994  $\mu$ s illumination time; (c) 500 Hz projection rate with 1994  $\mu$ s illumination time; (d) 2 kHz projection rate with 200  $\mu$ s illumination time; (e) 1 kHz projection rate with 300  $\mu$ s illumination time; (f) 500 Hz projection rate with 800  $\mu$ s illumination time.

### 3.3. Phase measurement error analysis

To visually justify the coupling effects, we did experiments by projecting fringe patterns with two different fringe pitches (18 pixels and 300 pixels). In these experiments, the camera was synchronized with the projector, and the exposure time of the camera was set to the maximum under different speeds (i.e., 494  $\mu$ s for 2 kHz, 994  $\mu$ s for 1 kHz, and 1994  $\mu$ s for 500 Hz). For the projector, we tested the same conditions as in Fig. 4. Fig. 5 shows the patterns captured under those different conditions. Specifically, Fig. 5(a)–(c) shows the patterns captured under different projection speeds of respectively 2 kHz, 1 kHz, and 500 Hz with the maximum illumination time. It clearly shows that the patterns overlap with their adjacent neighbors. Fig. 5(d)–(f) shows the corresponding patterns with a shorter illumination time. Unlike the previous case, these patterns are visibly unhindered, which means that the coupling effects are significantly alleviated.

To better view the difference between those patterns shown in Fig. 5, their corresponding cross sections are plotted as shown in Fig. 6. In Fig. 6(a) and (b), we can clearly see that there are wavelets overlapping the sinusoidal wave. From Fig. 6(c)–(f), the sinusoidal wave becomes smoother without any obvious overlapping wavelets.

### 3.4. Phase measurement error analysis

In order to test the performance of the DLP LightCommander projector, we carried out experiments to measure and analyze the phase error. A flat white board was used in this experiment. To obtain phase error, we first projected sinusoidal patterns one by one to ensure that there are no coupling issues, from which the reference phase was extracted. By comparing with the reference phase, we can obtain the phase error of the binary patterns under different conditions [21]. Fig. 7(a)–(c) shows the cross sections of the phase errors under 2 kHz, 1 kHz, and 500 Hz respectively with

the maximum illumination time. And the standard errors are respectively 0.176 rad, 0.067 rad, and 0.026 rad. Since the measured object is a flat board, the standard error represents the measurement accuracy. Fig. 7(d)–(f) shows the corresponding results with a shorter illumination time, while the standard errors are 0.018 rad, 0.019 rad, and 0.016 rad. We find that if the maximum illumination times are used, the phase error is large when the projection speeds are higher than 1 kHz. When the projection speeds are set to a comparably lower value (less than 500 Hz), the phase error decreases considerably. This is understandable since the transient response of the DMD has relatively less impact overall. In contrast, if a shorter illumination time is used, the phase error for all projection speeds is much smaller, with the higher speeds having larger reduction. For the 2 kHz projection speed, the phase error decreases by nearly 90% to a rms value of 0.018 rad, which is negligible even for high quality measurement.

### 3.5. 3D shape measurement for static object

To further verify the performance of the DLP LightCommander projector under different conditions, we carried out more experiments to measure the 3D shape of a static object. In this research, we adopted the same reference-plane-based calibration method as described in Ref. [8]. A 3D sculpture of a cat was measured and reconstructed under the same conditions experimented previously. Fig. 8(a) shows the photograph of the 3D sculpture. Fig. 8(b) shows a severely coupled pattern of 2 kHz with the maximum illumination time, while the corresponding pattern of 2 kHz with a shorter illumination time is shown in Fig. 8(c). By visually observing these patterns, we can clearly see the improvement brought about by reducing the illumination time.

Fig. 9(a)–(c) respectively shows the recovered 3D results of 2 kHz, 1 kHz, and 500 Hz with the maximum illumination time, while Fig. 9(d)–(f) shows the corresponding 3D results with a shorter illumination time. It should be noted that we use the same color to encode depth  $z$  from different data sets. Comparing the

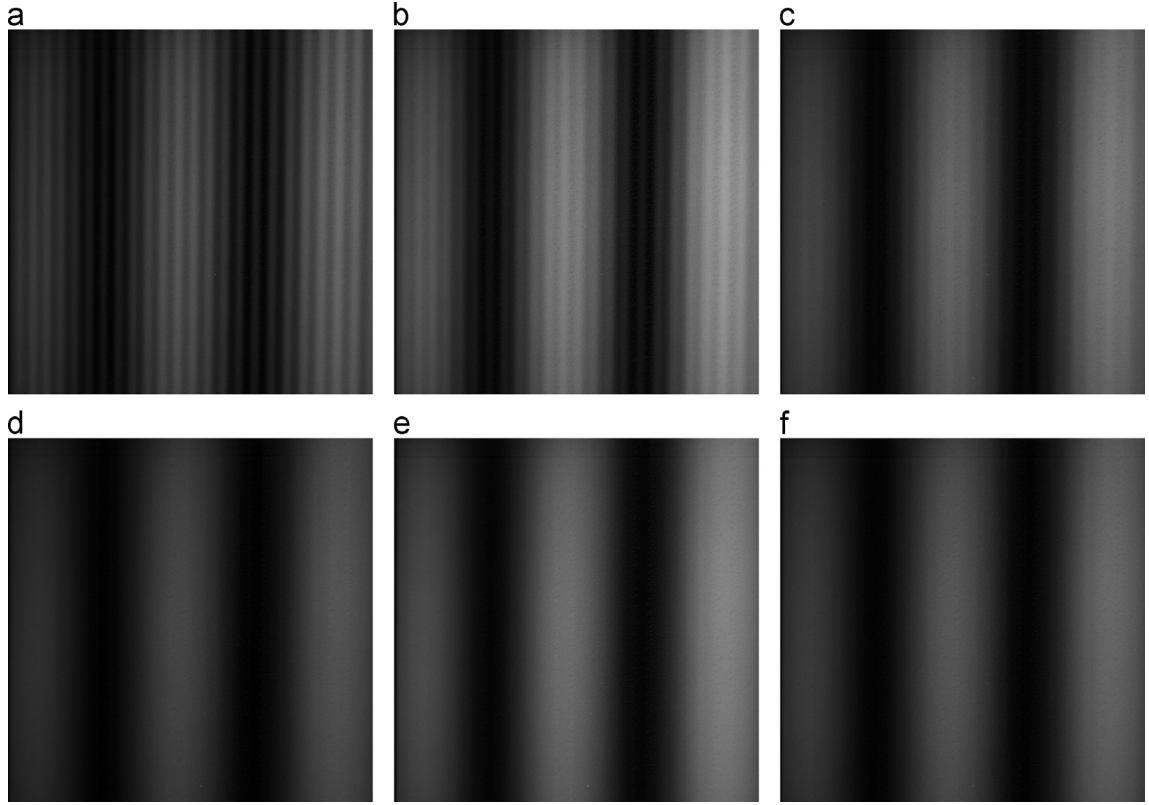


**Fig. 5.** Captured low spatial frequency fringe patterns that shows the coupling effect under different conditions. (a) 2 kHz projection rate with 494  $\mu$ s illumination time; (b) 1 kHz projection rate with 994  $\mu$ s illumination time; (c) 500 Hz projection rate with 1994  $\mu$ s illumination time; (d) 2 kHz projection rate with 200  $\mu$ s illumination time; (e) 1 kHz projection rate with 300  $\mu$ s illumination time; (f) 500 Hz projection rate with 800  $\mu$ s illumination time.

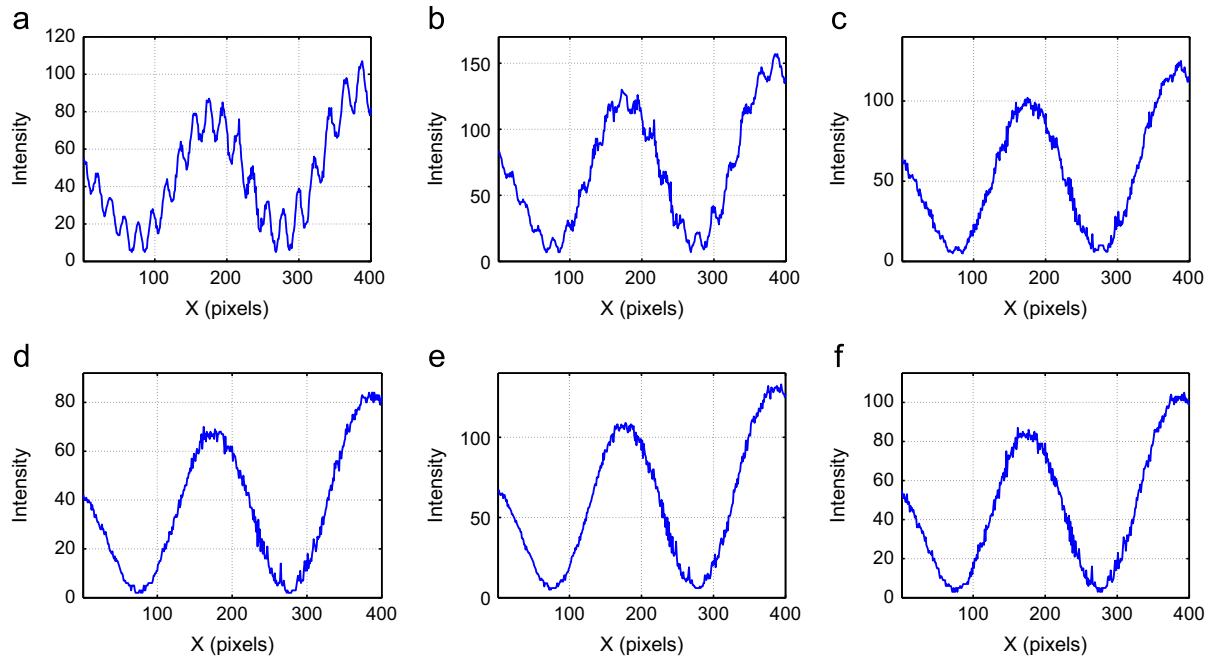


**Fig. 6.** Cross sections of the fringe patterns shown in Fig. 5. (a) 2 kHz projection rate with 494  $\mu$ s illumination time; (b) 1 kHz projection rate with 994  $\mu$ s illumination time; (c) 500 Hz projection rate with 1994  $\mu$ s illumination time; (d) 2 kHz projection rate with 200  $\mu$ s illumination time; (e) 1 kHz projection rate with 300  $\mu$ s illumination time; (f) 500 Hz projection rate with 800  $\mu$ s illumination time.

results among the figures in the first row where the projection illumination time is full, it can be found that the reconstructed surface becomes smoother when the projecting speed decreases. At approximately 500 Hz, the 3D result is already very good.

Meanwhile, by comparing the results in the first and the second row images, we can conclude that by using a shorter illumination time, the quality of the reconstructed 3D results are significantly improved for all different projection speeds, with higher speeds

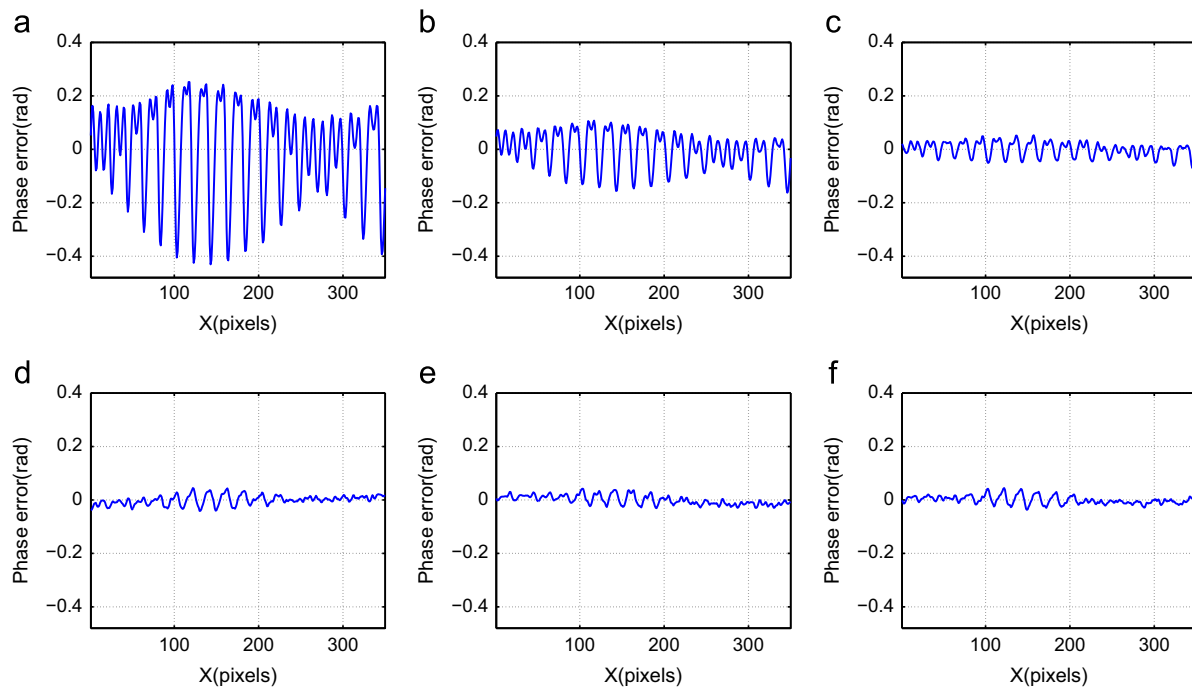


**Fig. 7.** Phase measurement error under different conditions. These figures show the same cross sections of the corresponding phase error maps. (a) 2 kHz projection rate with 494  $\mu$ s illumination time; (b) 1 kHz projection rate with 994  $\mu$ s illumination time; (c) 500 Hz projection rate with 1994  $\mu$ s illumination time; (d) 2 kHz projection rate with 200  $\mu$ s illumination time; (e) 1 kHz projection rate with 300  $\mu$ s illumination time; (f) 500 Hz projection rate with 800  $\mu$ s illumination time.

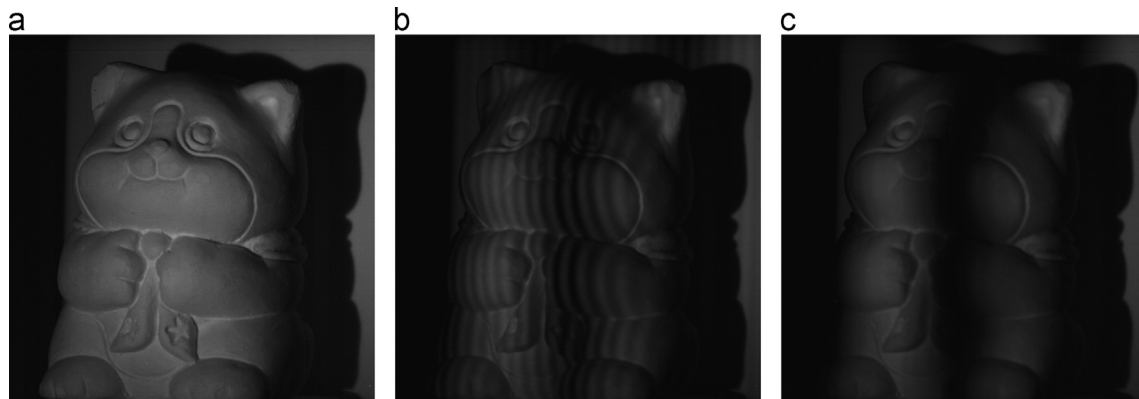


**Fig. 8.** Experimental results of a static object. (a) Photograph of the object; (b) captured fringe pattern with lower frequency for 2 kHz projection rate with 494  $\mu$ s illumination time; (c) captured fringe pattern with lower frequency for 2 kHz projection rate with 200  $\mu$ s illumination time.

having more improvement. This is consistent with our previous experimental findings. Therefore, we recommend that to measure static objects with high-quality, it is better to either lower the projection speed to 500 Hz or less and increase the illumination time, or shorten the illumination time and increase the projector speed.

### 3.6. Superfast 3D shape measurement

Since our ultimate goal is to mitigate the coupling effect of the DLP LightCommander projector for high-speed measurement, we conducted an experiment to capture and recover the motion of a pendular ball. In this experiment, a ball with a radius of about 43.6 mm is suspended by a string and released from the same height each time to ensure the motions are almost identical under varying projection and capture conditions. The important difference to keep in mind between this and the previous experiment is that the motion itself could also contribute to the phase measurement error. Fig. 10(a) shows the photograph of the pendular ball. Fig. 10(b) shows a severely coupled pattern of 2 kHz with the

maximum illumination time, while the corresponding pattern of 2 kHz with a shorter illumination time is shown in Fig. 10(c).

Fig. 11 as well as the associated medias (Media 1, Media 2, and Media 3; these medias can be downloaded from [http://www.vrac.iastate.edu/~song/OLEN\\_00934.zip](http://www.vrac.iastate.edu/~song/OLEN_00934.zip)) shows the 3D recovered results under different conditions. Fig. 11(a)–(c) shows the results of 2 kHz, 1 kHz and 500 Hz with the maximum illumination time, while Fig. 11(d)–(f) shows the corresponding results with a shorter illumination time, as used before. Comparing all the results in Fig. 11, we can clearly see that the best result is from 2 kHz with a shorter illumination time. All the other results have evident stripe noise on the recovered 3D surfaces. This finding is different from that of measuring a static object because the lower projection speed (less than 2 kHz) could have motion induced artifacts, as evident from these experimental results. 1 kHz capturing speed has some artifacts caused by motion, while the 500 Hz capturing speed has more motion artifacts, albeit the error caused by motion and the error caused by coupling appear to be similar. The similarity between these two artifacts actually made the coupling problem more difficult to be identified and solved since the

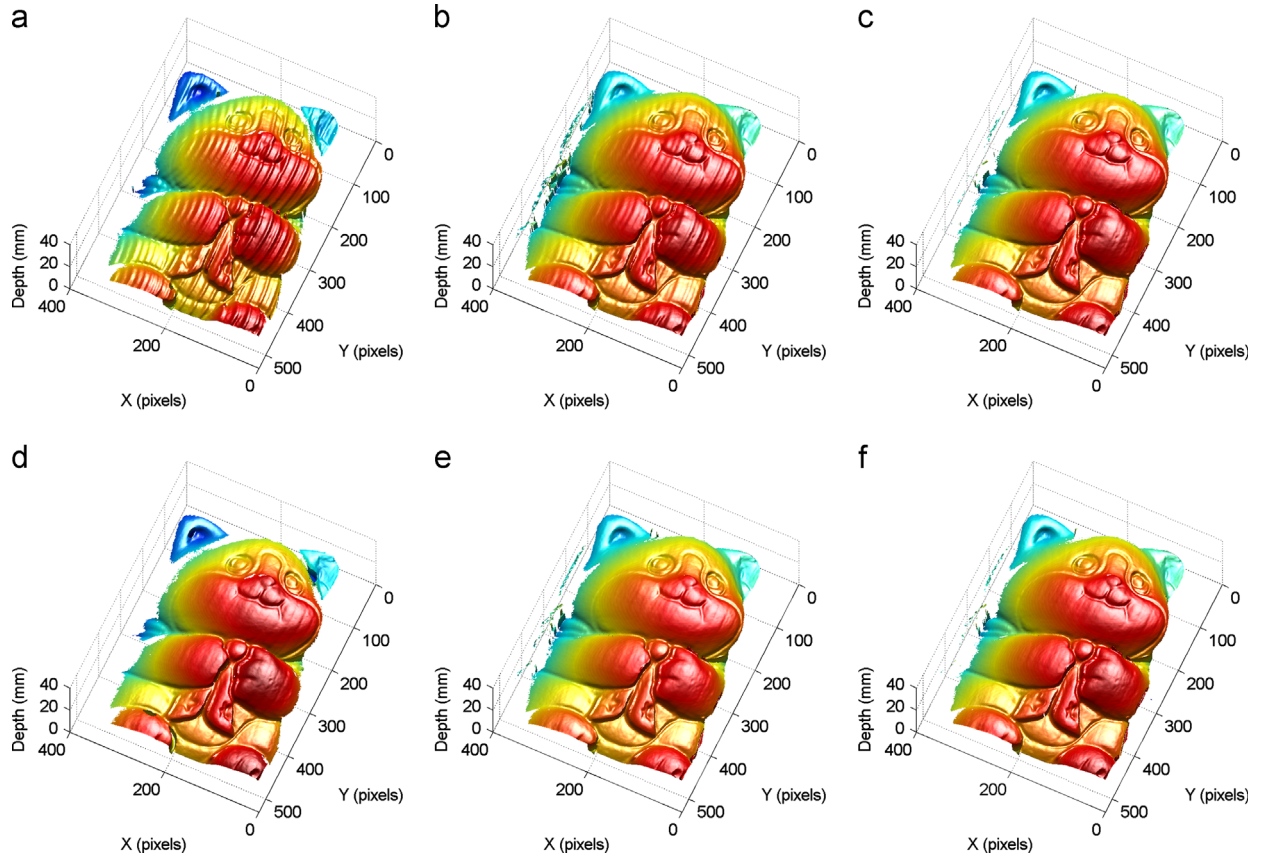


**Fig. 9.** 3D shape measurement results of the sculpture shown in Fig. 10 under different conditions. (a) 2 kHz projection rate with 494  $\mu$ s illumination time; (b) 1 kHz projection rate with 994  $\mu$ s illumination time; (c) 500 Hz projection rate with 1994  $\mu$ s illumination time; (d) 2 kHz projection rate with 200  $\mu$ s illumination time; (e) 1 kHz projection rate with 300  $\mu$ s illumination time; (f) 500 Hz projection rate with 800  $\mu$ s illumination time. (For interpretation of the references to color in this figure caption, the reader is referred to the web version of this article.)

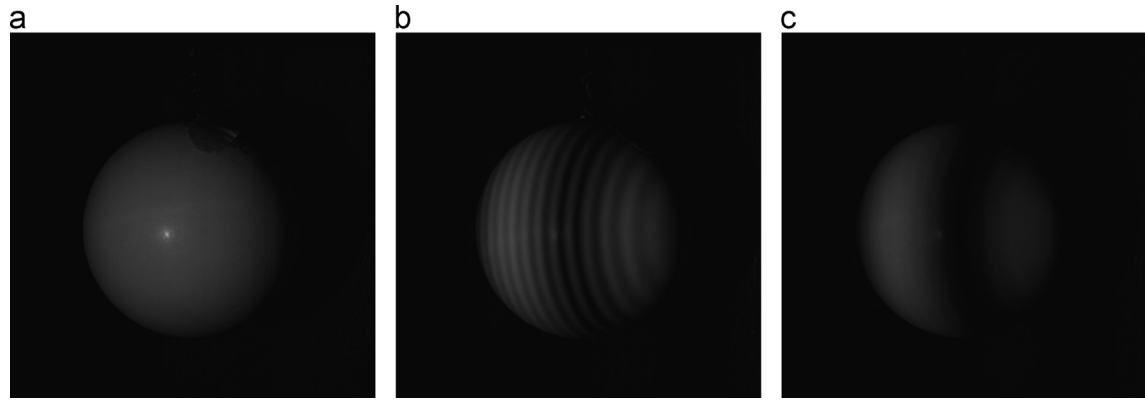


**Fig. 10.** Experimental results of a pendular ball. (a) Photograph of the ball; (b) captured fringe pattern with lower frequency for 2 kHz projection rate with 494  $\mu$ s illumination time; (c) captured fringe pattern with lower frequency for 2 kHz projection rate with 200  $\mu$ s illumination time.

motion-induced artifact is well known and easy to be responsible for this type of error. Therefore, we recommend that to capture high-speed motion, a good solution is to use a shorter illumination time with a high speed instead of lowering the projection speed due the motion artifacts.

#### 4. Conclusions

This paper has presented the limitation of the DLP LightCommander projector when operated under high speeds. It specifically looked into the transient effect of the DMD response on phase measurement quality when binary structured patterns

are used. We find that the coupling effect influences the measurements significantly especially when the projection speed is higher than 1 kHz. By lowering the projection speed, considerably better results can be obtained for static or slow-speed objects measurement. In order to capture highly dynamic events or objects, a high projection speed is required, coupled with a shorter illumination time for the projector. Experimental results of both static and high-speed moving objects were presented and verified the success of the proposed method.

It is important to note that not only the DLP LightCommander projector has the issues we discovered, our research also found that the newer versions high-speed DLP projectors (i.e., DLP LightCrafter 3000 and DLP LightCrafter 4500) also have the same



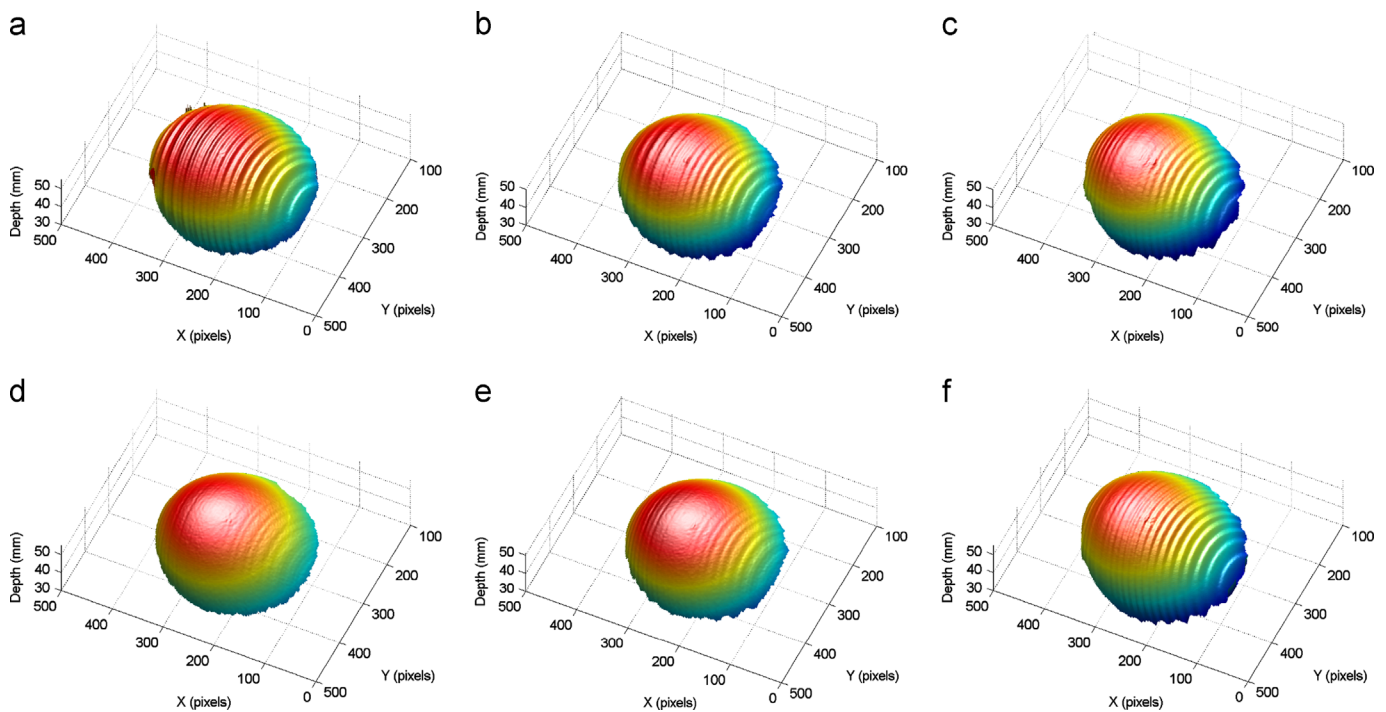


**Fig. 11.** 3D shape measurement results of a moving pendular ball under different conditions. (a) 2 kHz projection rate with 494  $\mu$ s illumination time; (b) 1 kHz projection rate with 994  $\mu$ s illumination time; (c) 500 Hz projection rate with 1994  $\mu$ s illumination time; (d) 2 kHz projection rate with 200  $\mu$ s illumination time; (e) 1 kHz projection rate with 300  $\mu$ s illumination time; (f) 500 Hz projection rate with 800  $\mu$ s illumination time. (Media 1 for (a) and (d), Media 2 for (b) and (e), Media 3 for (c) and (f)).

problems, albeit at different significance levels. We verified that the method presented in this paper could also be applied to those projectors to solve such similar issues.

## Acknowledgments

This material is based upon work sponsored by the Deere & Co. Any opinion, findings, and conclusions or recommendations expressed in this paper are those of the authors and do not necessarily reflect the views of the Deere & Co.

## References

- [1] Wang Y, Laughner JI, Efimov IR, Zhang S. 3D absolute shape measurement of live rabbit hearts with a superfast two-frequency phase-shifting technique. *Opt Express* 2013;21(5):5632–822.
- [2] Zhang S. Recent progresses on real-time 3-D shape measurement using digital fringe projection techniques. *Opt Laser Eng* 2010;48(2):149–58.
- [3] Li Y, Zhao C, Qian Y, Wang H, Jin H. High-speed and dense three-dimensional surface acquisition using defocused binary patterns for spatially isolated objects. *Opt Express* 2010;18 21,628–635.
- [4] Schaffer M, Große M, Harendt B, Kowarschik R. Coherent two-beam interference fringe projection for high speed three-dimensional shape measurements. *Appl Opt* 2013;52:2306–11.
- [5] Heist S, Sieler M, Breitbarth A, Khmstedt P, Notni G. High-speed 3D shape measurement using array projection. In: *Proceedings of the SPIE*; 2013. p. 878, 815–11.
- [6] Zhang S, van der Weide D, Oliver J. Superfast phase-shifting method for 3-D shape measurement. *Opt Express* 2010;18(9):9684–9.
- [7] Lei S, Zhang S. Flexible 3-D shape measurement using projector defocusing. *Opt Lett* 2009;34(20):3080–2.
- [8] Xu Y, Ekstrand L, Dai J, Zhang S. Phase error compensation for three-dimensional shape measurement with projector defocusing. *Appl Opt* 2011;50(17):2572–81.
- [9] Yoshizawa T, Fujita H. Liquid crystal grating for profilometry using structured light. In: *Proceedings of the SPIE*, vol. 6000. Boston, MA; 2005. p. 60, 000H1–10.
- [10] Fujita H, Yamatan K, Yamamoto M, Otani Y, Suguro A, Morokawa S, et al. Three-dimensional profilometry using liquid crystal grating. In: *Proceedings of the SPIE*, vol. 5058. Beijing, China; 2003. p. 51–60.
- [11] Wang Y, Zhang S. Optimum pulse width modulation for sinusoidal fringe generation with projector defocusing. *Opt Lett* 2010;35(24):4121–3.
- [12] Ajubi GA, Ayubi JA, Martino JMD, Ferrari JA. Pulse-width modulation in defocused 3-D fringe projection. *Opt Lett* 2010;35:3682–4.
- [13] Zuo C, Chen Q, Feng S, Feng F, Gu G, Sui X. Optimized pulse width modulation pattern strategy for three-dimensional profilometry with projector defocusing. *Appl Opt* 2012;51(19):4477–90.
- [14] Zuo C, Chen Q, Gu G, Feng S, Feng F, Li R, et al. High-speed three-dimensional shape measurement for dynamic scenes using bi-frequency tripolar pulse-width-modulation fringe projection. *Opt Laser Eng* 2013;51(8):953–60.
- [15] Xian T, Su X. Area modulation grating for sinusoidal structure illumination on phase-measuring profilometry. *Appl Opt* 2001;40(8):1201–6.
- [16] Lohry W, Zhang S. 3D shape measurement with 2D area modulated binary patterns. *Opt Laser Eng* 2012;50(7):917–21.
- [17] Wang Y, Zhang S. Three-dimensional shape measurement with binary dithered patterns. *Appl Opt* 2012;51(27):6631–6.
- [18] Lohry W, Zhang S. Genetic method to optimize binary dithering technique for high-quality fringe generation. *Opt Lett* 2013;38(4):540–2.
- [19] Dai J, Li B, Zhang S. High-quality fringe patterns generation using binary pattern optimization through symmetry and periodicity. *Opt Laser Eng* 2014;52:195–200.
- [20] Malacara D, editor. *Optical shop testing*, 3rd ed. New York: John Wiley and Sons; 2007.
- [21] Wang Y, Zhang S. Comparison among square binary, sinusoidal pulse width modulation and optimal pulse width modulation, methods for three-dimensional shape measurement. *Appl Opt* 2012;51(7):861–72.